be of similar magnitude. Although there are no experimental data available for these particular systems, the results of our ab initio molecular orbital calculations largely support the notion that σ effects here are not of primary importance.

References and Notes

(1) (a) University of California, Alfred P. Sloan Fellow 1974–1976; (b) Carnegie-Mellon University; (c) Université Pierre and Marie Curie.
(2) (a) D. R. Herschbach and L. C. Krisher, *J. Chem. Phys.*, **28**, 728 (1958).
(3) (a) J. E. Kilpatrick and K. S. Pitzer, *J. Res. Nat. Bur. Stand.*, **37**, 163 (1946); (b) D. R. Lide, Jr., and D. E. Mann, *J. Chem. Phys.*, 27, 868 (1957); (c) W. G. Fateley and F. A. Miller, *Spectrochim. Acta*, **19**, 611 (1963); (d) E. Hirota, *J. Chem. Phys.*, **45**, 1984 (1966); (e) K. D. Möller, A. R. DeMeo, D. R. Smith, and L. H. London, *ibid.*, **47**, 2609 (1967).
(4) (a) R. W. Kilb, C. C. Lin, and E. B. Wilson, Jr., *J. Chem. Phys.*, **26**, 1695 (1957); (b) D. R. Herschbach, *ibid.*, **31**, 91 (1959).
(5) T. N. Sarachman, *J. Chem. Phys.*, **49**, 3146 (1968).
(6) (a) W. J. Hehre and L. Salem, *J. Chem. Soc., Chem. Commun.*, 754 (1973); (b) D. Cremer, J. S. Binkley, J. A. Pople, and W. J. Hehre, *J. Am. Chem. Soc.*, **96**, 6900 (1974).
(7) (a) J. P. Lowe, *J. Am. Chem. Soc.*, **92**, 3799 (1970); (b) N. D. Epiotis, *ibid.*, **95**, 3087 (1973).
(8) For a description of the valence orbitals on a methyl group see (a) R. Hoffmann, *Pure Appl. Chem.*, **24**, 567 (1970); (b) B. M. Gimarc, *J. Am. Chem. Soc.*, **93**, 593 (1971); (c) R. Hoffmann, L. Radom, J. A. Pople, P. v. R. Schleyer, W. J. Hehre, and L. Salem, *ibid.*, **94**, 6221 (1972); (d) B. M. Gimarc, *Acc. Chem. Res.*, 7, 384 (1974).
(9) Upon interaction, energy levels split; one is lowered the other raised to a larger extent. Hence, if in total two electrons are involved (interaction between filled and empty orbitals) net stabilization results. If, however, both interacting levels are doubly occupied, destabilization results. For a discussion see R. Hoffmann, *Acc. Chem. Res.*, **4**, 1 (1971).
(10) For examples of conformational changes resulting from electronic excitation see A. J. P. Devaquet, R. E. Townshend, and W. J. Hehre, *J. Am. Chem. Soc.*, submitted.
(11) R. Ditchfield, W. J. Hehre, and J. A. Pople, *J. Chem. Phys.*, **54**, 724 (1971).
(12) J. A. Pople and M. Gordon, *J. Am. Chem. Soc.*, **89**, 4253 (1967).
(13) W. J. Hehre, R. F. Stewart, and J. A. Pople, *J. Chem. Phys.*, 51, 2657 (1969).
(14) W. J. Hehre, W. A. Lathan, R. Ditchfield, M. D. Newton, and J. A. Pople, Program no. 236, Quantum Chemistry Program Exchange, Indiana University, Bloomington, Ind.
(15) K. V. L. N. Sastry and R. F. Curl, Jr., *J. Chem. Phys.*, **41**, 77 (1964).
(16) J. Meier, A. Bauder, and Hs. H. Günthard, *J. Chem. Phys.*, **57**, 1219 (1972).
(17) W. J. Hehre and P. C. Hiberty, *J. Am. Chem. Soc.*, **96**, 2665 (1974).
(18) For a discussion of the cyclopropane Walsh orbitals see R. Hoffmann and R. B. Davidson, *J. Am. Chem. Soc.*, **93**, 5699 (1971).
(19) W. J. Hehre and J. A. Pople, *J. Am. Chem. Soc.*, **97**, 6941 (1975).
(20) A referee has commented that these same arguments should be able to account for the observed increase in the barrier to methyl rotation in 1-fluoropropene, relative to that in propene itself. This is indeed the case, as the effect of replacing one of the hydrogens on, say, ethylene by a fluorine atom is a polarization of the π system in the direction.

See ref 12 and 21 for a discussion.
(21) (a) W. J. Hehre and J. A. Pople, *J. Am. Chem. Soc.*, **92**, 2191 (1970); (b) W. J. Hehre, L. Radom, and J. A. Pople, *ibid.*, **94**, 1496 (1972).

Photoelectron Spectra and Molecular Properties. LI.[1-3] Ionization Potentials of Silanes Si_nH_{2n+2}

H. Bock,*[4a] W. Ensslin,*[4b] F. Fehér,*[4c] and R. Freund*[4c]

Contribution from the Institutes of Inorganic Chemistry, University of Frankfurt, Frankfurt, Germany, and University of Cologne, Cologne, Germany.

Received December 30, 1974

Abstract: The low-energy photoelectron spectra (PES) of silanes Si_nH_{2n+2} (n = 1-5) are reported. Their assignment is achieved by spectral comparison, by parametrization of MO models using PES data, and by modified CNDO calculations, which have been used in addition to examine the conformational dependence of the ionization potentials. The unsymmetrical splitting pattern observed in the σ_{SiSi} ionization region of the silane PES stimulates a rediscussion of bond-bond interaction models for permethylated silanes or alkanes.

Photoelectron spectra (PES) of permethylated linear and cyclic silanes display isolated bands in the 8-10 eV region, which are readily assigned to ionizatiions from the silicon framework.[5] The corresponding spectroscopic splitting patterns can be rationalized within a simple LCBO (linear combination of bond orbitals) model, which only considers the silicon bonds and their topology as shown in Figure 1.

Assuming validity of Koopmans theorem,[6] $IE_n = -\epsilon_j^{SCF}$, and some approximate proportionality, $\epsilon_j^{SCF} \propto \epsilon_j^{HMO}$, the linear regression of Figure 1 yields the parameters α^R_{SiSi} = 8.7 eV and $\beta^R_{SiSi/SiSi}$ = 0.5 eV.[5] Extended models, incorporating the unoccupied molecular orbitals, render possible an understanding of other properties of the alkylsilanes, e.g., the decrease in first excitation energies with increasing silicon chain length[7] or the ESR spectra of their radical anions.[8] Nevertheless, the neglect of the methyl groups in a simplifying bonding model for methylsilanes $-[Si(CH_3)_2]_n-$ (Figure 1) needs further elaboration.

Hydrocarbons C_nH_{2n+2} have been repeatedly investigated using photoelectron spectroscopy, e.g.,[9-12] and analogous bonding models[12-16] seem well-suited to interpret many of their molecular properties. Although alkanes are smaller in molecular size than corresponding methyl silanes of the same chain length, n, in general numerous bands overlap in their PES and often render difficult unequivocal assignments[9-12] as well as comparative discussion.[12] The PES of silanes Si_nH_{2n+2} (n = 1,[9,17,18] 2,[9] 3, 4, 5) have been recorded, because increased PE band separation and consequently more obtrusive assignment were expected, shedding more light also on the applicability of bond orbital models to both methyl silanes as well as alkanes.

Experimental Section

Preparation and Purification of Silanes. The silanes Si_nH_{2n+2} (n = 2, 3, 4, and 5) have been prepared—in the course of investigations to determine their molecular properties[2]—by a technical scale hydrolytic decomposition of 160 kg of Mg_2Si[19] with diluted phosphoric acid,[20] yielding 5 l. of a mixture containing, among other isomers as well as higher silanes, 5.5% disilane, 34.8% trisilane, 29.2% n-tetrasilane, and 15.5% n-pentasilane. The rather dangerous mixture of the gaseous hydrolysis products, monosilane, hydrogen, and uncondensed disilane was cautiously blown off via a water siphon. Separation and purification of the liquid silanes were achieved by fractionate distillation over a 1.5-m column filled with

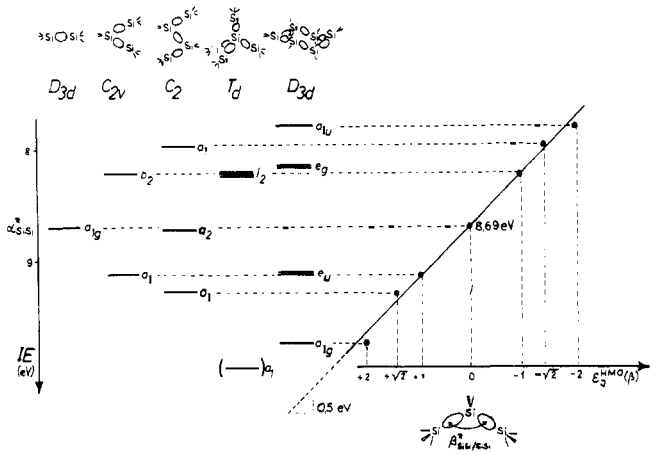

Figure 1. Correlation between σ_{SiSi} ionization potentials, IP_n (eV) of permethylated silanes and Huckel orbital eigenvalues ϵ_J^{HMO}.

4-mm metal spirals and preparative GC[21] with a final purity >99%.

Recording of the Photoelectron Spectra. With regard to the extreme oxygen sensitivity of silanes, all samples were handled using a special technique;[22] the reagent flasks were sealed with plastic caps and the liquid silanes transferred under normal pressure using syringes with needles covered with sliding plastic protection caps. All glassware including the small vacuum line connected to the spectrometer was repeatedly evacuated and flushed with prepurified nitrogen. After injection into the photoelectron spectrometer vacuum line the liquid silanes were frozen out by cooling with liquid nitrogen, the system was evacuated by the spectrometer pumps, and the samples were allowed to warm up. The vapor pressure at room temperature, e.g., for *n*-pentasilane 3 Torr at 20°C,[23] permits recording of the PES. Gaseous disilane was directly fed into the spectrometer from a steel cylinder via a vacuum-tight depressurizer valve and the evacuated vacuum line. Excess silane condensed at the spectrometer cooling trap (−196°C), which—to avoid collection of larger silane quantities—was exchanged from time to time and allowed to warm up, thereby permitting a harmless burn-off of the silanes. All PES were calibrated using argon (15.76 eV), the half-bandwidth has usually been 20–25 meV.

Calculations. A modified CNDO version[24] without 3d orbitals in the basis set[25] was used, reparametrized to improve correlations $\Delta IE_{i,j} \approx \Delta\epsilon_{i,j}^{SCF}$ between differences in PE ionization potentials and differences in orbital energies.[6] To examine the conformational dependence of ionization potential differences, a PES simulation program[3] has been developed on the following assumptions. (i) A reasonable reproduction of silane PE bands can be achieved by placing Lorentz curves[26] around the calculated eigenvalues, if the half-bandwidths are adjusted according to

$$X_{1/2} = X_{1/2}(\mathrm{PE})\frac{\Delta\epsilon_{i,j}^{SCF}}{\Delta IE_{i,j}} \qquad (1)$$

$X_{1/2}$(PE) being the experimental half-bandwidth of the isolated first PE band of disilane (Figure 2). The procedure was tested with good results for *n*-trisilane.[3] (ii) Only staggered conformations need to be taken into account (rotational barrier of disilane 1.1 kcal/mol; see ref 27). (iii) The ratio of individual conformers, i.e., anti:gauche, for *n*-tetrasilane (Figure 7) may be approximated judging from best fit of a simulated to the experimental PES, achieved by "trial and error" composition of weighted contributions of individual conformer spectra.[3] The conformer ratio thus obtained is not changed on inclusion of 3d orbitals into the basis set.[3,27]

PES of Silanes and Assignment

The PES of silanes Si_nH_{2n+2}, recorded under precautions as specified in the experimental section, are shown in Figure 2; their observable vertical ionization energies are summarized in Table I. Starting with the PES of monosilane SiH_4[9,17,18] (Figure 2), for its eight valence electrons four ionization energies are expected and found, split according

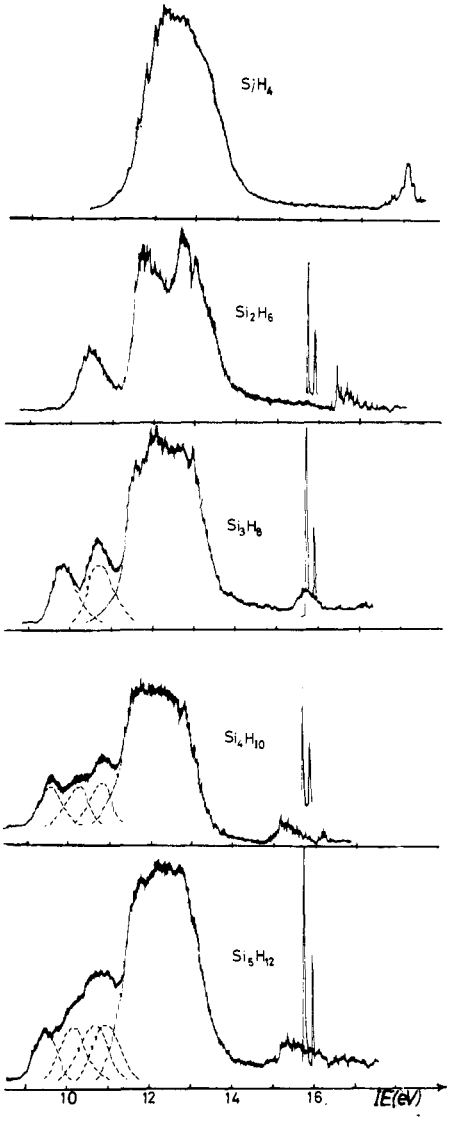

Figure 2. PES of SiH_4[9,17,18] and linear silanes Si_nH_{2n+2} (n = 2, 3, 4, 5).

to the T_d molecular symmetry into a threefold "t_2" and a single a_1 band. The triple degeneracy of the molecular orbitals is removed on ionization, i.e., the resulting T_2 radical cation states are split by a $T_d \rightarrow D_{2d}$ Jahn-Teller distortion,[9] and therefore the first PE band between 11.5 and 14 eV appears considerably broadened. The other PE band centered at 18.16 eV is assigned to electron removal from the a_1 molecular orbital with predominant $3s_{Si}$ contribution, in accord with the observed vibrational fine structure.[9,17]

Comparison with the PES of the higher linear silanes (Figure 2) results in an immediate classification of ionization regions. Thus by analogy to SiH_4, the more or less structured band humps between 11.5 and 14 eV are readily assigned to ionization from orbitals with σ_{SiH} main contribution. At higher energy other PE bands are visible, the low intensity of which is partly spectrometer dependent and partly can be explained by a smaller helium(I) cross-section of $3s_{Si}$ electrons. Particularly interesting are the PE band splitting patterns below 11 eV: extending in front of the "σ_{SiH} mountain" n bands are observed for the higher silanes $H_3Si(SiH_2)_nH$ with n = 2, 3, 4 (Figure 2); thereby the maxima for n = 3, 4 have to be extracted by deconvolution (Table I). Following the above argumentation, these bands have to be assigned inevitably to electron explusion from orbitals with predominant σ_{SiSi} contribution.

Table I. Vertical Ionization Potentials[a] of Linear Silanes Si_nH_{2n+2} (n = 2, 3, 4, 5)

Compound	σ_{SiSi} 1	2	3	4	σ_{SiH}	"Si_{3s}"
Si_2H_6	10.53				(11.9) (12.1) 12.73 13.08	16.5
Si_3H_{10}	9.87	10.72			(11.65) (12.02) (12.17) (12.8) (13.02)	15.7
n-Si_4H_{10}	9.62	(10.3)	10.8_5		(11.6) (11.8) (12.0) (12.4) (12.92)	15.3 16.3
n-Si_5H_{12}	9.36	(10.1)	(10.6)	(10.9)	(11.8) (12.2) (12.5) (12.7)	15.3

[a] Parentheses ( ) connote strongly overlapping bands.

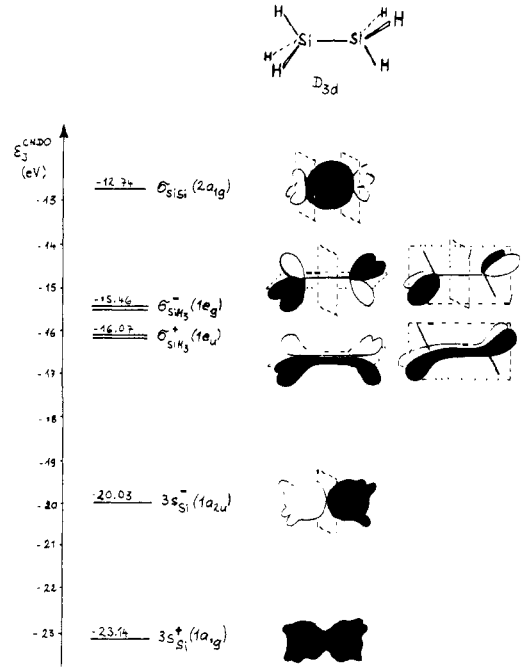

Figure 3. CNDO orbital sequence and orbital sketches for disilane.

Disilane. According to electron diffraction[28] the preponderant conformer is the staggered one, and for D_{3d} molecular symmetry the seven occupied molecular orbitals are predicted to belong to the representations $\Gamma = 2a_{1g} + 1e_g + 1e_u + 1a_{2u}$. The orbital sequence may be gathered from Figure 3, which summarizes results of a modified CNDO calculation.

Judging from the "$3s_{Si}$" ($1a_{1g}$) CNDO eigenvalue (Figure 3), the corresponding highest valence electron ionization energy is expected near the helium(I) measurement border line of 21.21 eV. It can be approximated from the silane a_1 ionization at 18.16 eV assuming symmetrical split into both $1a_{1g}$ and $1a_{2u}$ orbitals by $IE(Si_2H_6{:}1a_{1g}) = IE(SiH_4{:}a_1) + |IE(SiH_4{:}a_1) - IE(Si_2H_6{:}a_{2u})| = 18.16 + (18.16 - 16.48) = 19.84$ eV. The other occupied orbital of same symmetry, $2a_{1g}$, obviously corresponds to the lowest $IE = 10.53$ eV and represents largely the σ_{SiSi} bond. Because of the considerable distance $1a_{1g}$-$2a_{1g}$ the σ_{SiSi} orbital should contain only small $3s_{Si}$ contributions and the CNDO calculation suggests prevailing $3p_{Si}$ character. The mean value of the remaining ionizations $|IE(1e_g) - IE(1e_u)|/2 = 12.46$ eV (Table I) may be taken as coulomb parameter α_{SiH_3} for pseudo π_{SiH_3} orbitals[25] (but cf. Figure 9).

Trisilane. Assuming C_{2v} molecular symmetry, the ten occupied molecular orbitals of trisilane are distributed among the following symmetry species: $\Gamma = 4a_1 + 1a_2 + 2b_1 + 3b_2$. To facilitate comprehension, sketches of the CNDO orbitals are presented in Figure 4. Within the MO model (Figure 4), the SiSi bonds can be identified to some extent with the two upper orbitals $3b_2$ and $4a_1$. However, due to

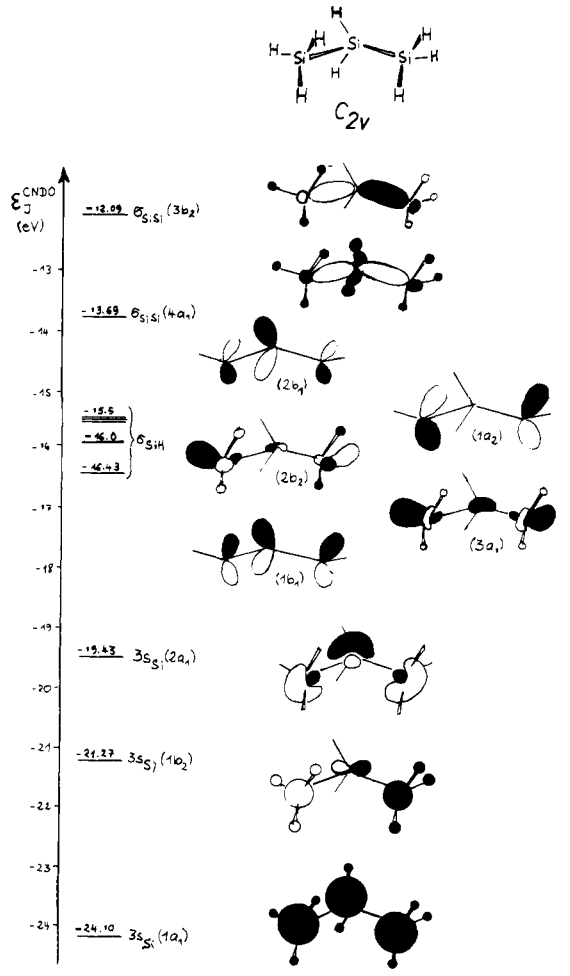

Figure 4. CNDO orbital sequence and orbital sketches for trisilane.

σ_{SiH} orbitals of same symmetry the admixture of SiH contributions has to be taken into account. The five σ_{SiH} type orbitals are calculated quite close to each other; in the trisilane PES (Figure 2) the corresponding bands overlap strongly to form the "σ_{SiH} mountain".

***n*-Tetrasilane and *n*-Pentasilane.** Expectedly, the $\sigma_{SiSi}/\sigma_{SiH}$ mixing increases with molecular size, i.e., an increasing number of orbitals of same symmetry, and with decreasing orbital distance. Mixing reaches a maximum in conformations of low molecular symmetry. In the case of *n*-tetrasilane, rotation around the central silicon-silicon bond leads to two energetically favored rotamers with staggered bonds. Schematic CNDO orbital diagrams (Figure 5) demonstrate increasing σ_{SiH} admixture to the σ_{SiSi} type orbitals with increasing negative orbital energy. The CNDO correlation diagram (Figure 5) also illustrates the considerable σ_{SiSi} orbital shifts depending on changes in bonding or antibonding interactions between silicon-silicon bonds with varying dihedral angle ω. Analogous, though less transparent, orbital shifts are calculated for rotations around the two central SiSi bonds of *n*-pentasilane (Figure 6). For a

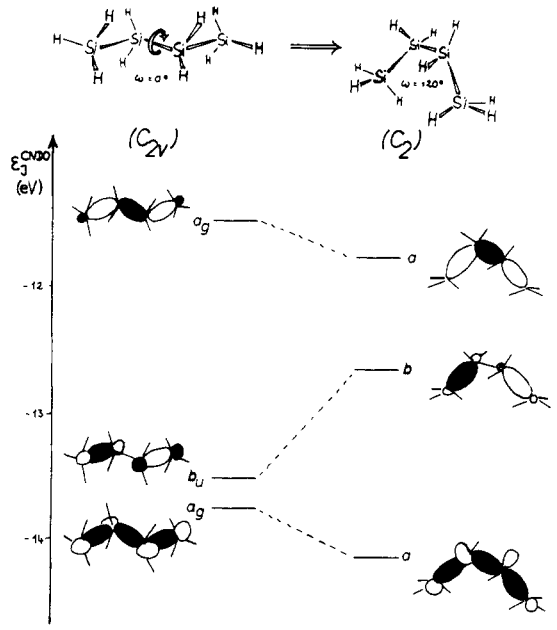

Figure 5. CNDO correlation diagram for the σ_{SiSi} orbitals of staggered *n*-tetrasilane rotamers.

rationalization of the individual orbital movements in Figure 6, one starts advantageously from the C_1 conformation with one SiSi bond twisted by $\omega = 120°$ out of the molecular plane, which is crossed in both rotations, $C_{2v} \rightarrow C_2$ as well as $C_{2v} \rightarrow C_s$, respectively (Figure 6). Again the orbital sketches illustrate that σ_{SiH} admixture increases with increasing negative eigenvalue and particularly in conformations of low symmetry. Thus on rotation $C_s \rightarrow C_1$ numerous changes in orbital sequence take place, traceable to the noncrossing rule between correlation lines of the same symmetry, and further illustrating the strong mixing of all orbitals in the C_2 conformation of *n*-pentasilane.

Alkanes and their derivatives probably exist in conformer mixtures as proven, e.g., for pent-1-yne by a microwave study,[29] according to which the gauche methyl form is slightly more stable than the trans methyl form. Inferring from the smaller rotational barrier of disilane[27] (~1.1 kcal/mol) relative to that of ethane[30] (~2.88 kcal/mol), *n*-tetrasilane and *n*-pentasilane might exist in conformer mixtures under measurement conditions. If so, then the PES (Figure 2) are superpositions of the spectra of the individual conformers. This speculation is at least in accord with a PES simulation, which starts from CNDO eigenvalues of the different staggered conformers, circumscribes Lorentz curves, and sums up according to weighted contributions of the conformers (see experimental section). Figure 7 shows

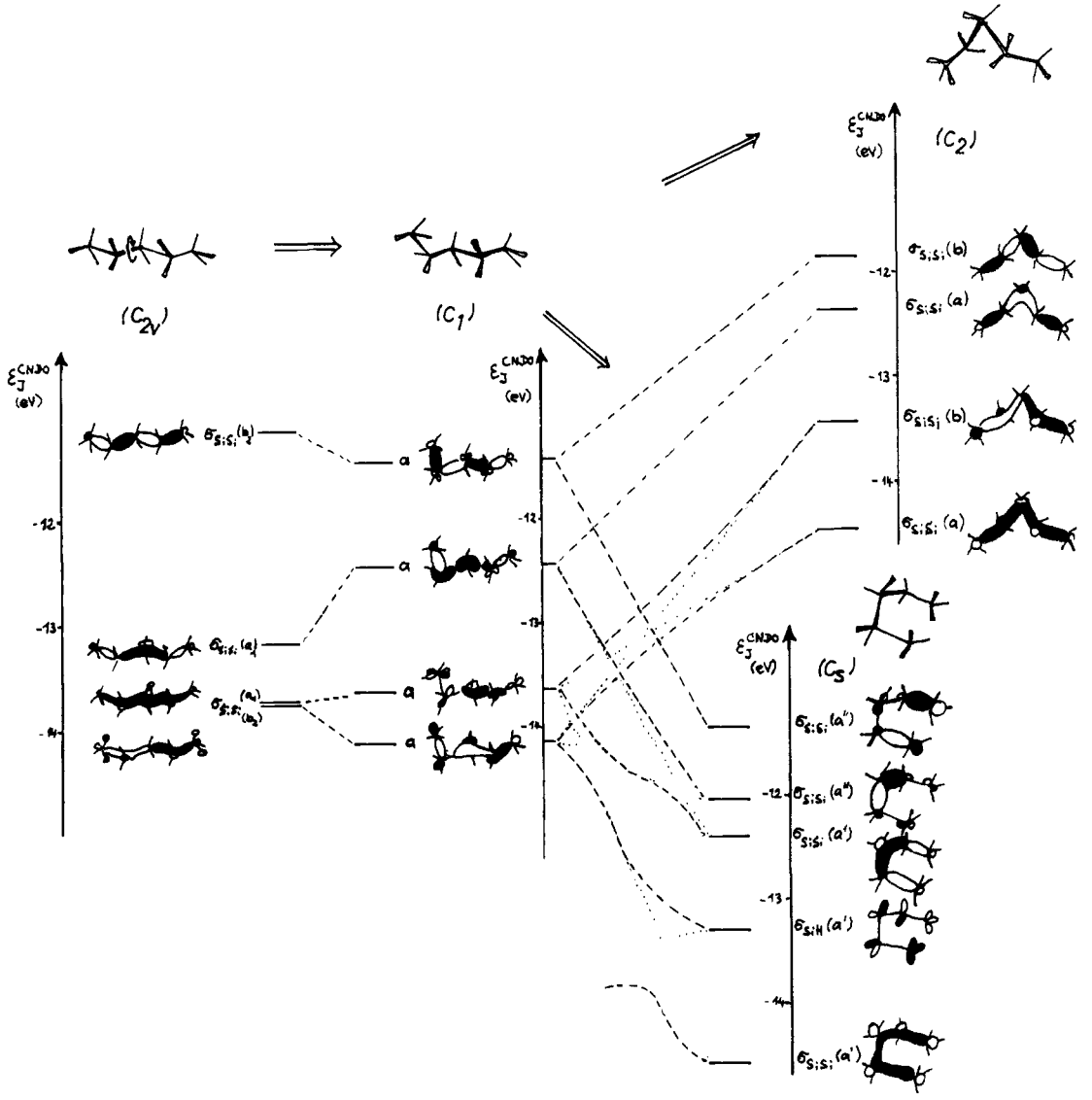

Figure 6. CNDO correlation diagram for the σ_{SiSi} orbitals of staggered *n*-pentasilane rotamers.

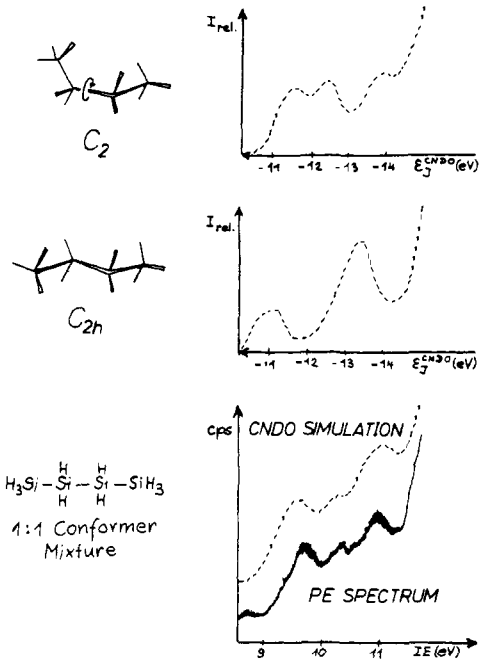

Figure 7. Simulated PES (8.5-11.5 eV) of anti and gauche *n*-tetrasilane conformers and their 1:1 superposition compared to the experimental PES.

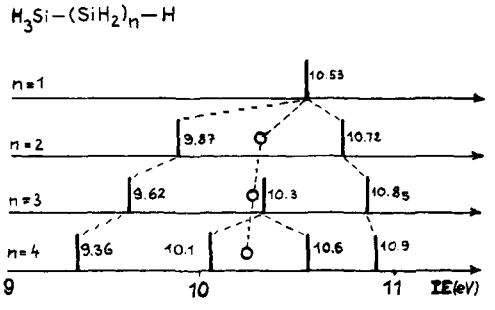

Figure 8. σ_{SiSi} ionization splitting patterns of silanes.

for the σ_{SiSi} ionization region of *n*-tetrasilane the simulated spectra of both anti (C_{2h}) and gauche (C_2) conformers (Figure 5) and their 1:1 superposition, which gives a reasonable fit to the recorded PES (Figure 7). Although conformational ambiguity possibly must be taken into consideration for both Si_4H_{10} and Si_5H_{12}, nevertheless, the above detailed assignment further confirms the initial approximate classification into σ_{SiSi}, σ_{SiH}, and $3s_{Si}$ ionization regions in the silane PES.

Discussion

SiSi Bond Ionizations. The PE spectroscopic splitting patterns of the silanes Si_nH_{2n+2} in the σ_{SiSi} ionization region below 11.5 eV, partly determined by band deconvolution (Figure 2 and Table I), are compared in Figure 8. Overlapping bands were deconvoluted (cf. experimental part: calculations) using the shape of the well-separated bands of di- and trisilane (Figure 2). The σ_{SiSi} ionization energies of silanes Si_nH_{2n+2} (Figure 8) demonstrate that there is no symmetrical split around the disilane value $IE_1(Si_2H_6) \equiv -\alpha^H{}_{SiSi}$ as observed for the methylsilanes $Si_n(CH_3)_{2n+2}$ around $IE_1(Si_2(CH_3)_6) \equiv -\alpha^{CH_3}{}_{SiSi}$ (Figure 1); the center of gravity $IE_n(\sigma_{SiSi})$ (Figure 8: O) moves to lower energies instead. The compression becomes especially evident for *n*-pentasilane with $IE_2 - IE_1 = 0.7$ eV $\gg$ $IE_4 - IE_3 = 0.35$ eV. For *n*-tetrasilane $IE_2 = 10.3$ eV deviates not only from the mean $IE_n(\sigma_{SiSi})$ but also from $IE_1(Si_2H_6) = 10.53$ eV (Figure 1). No doubt concerning

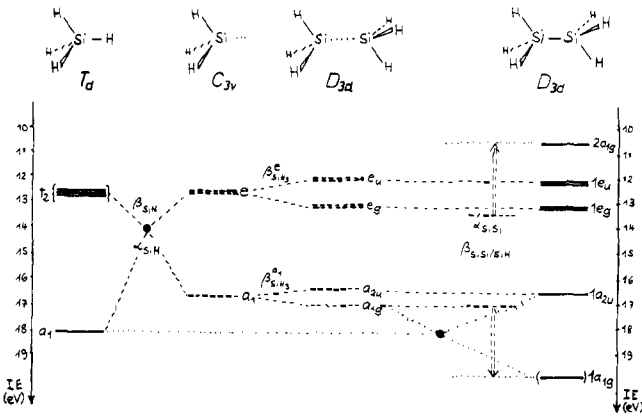

Figure 9. Complete LCBO MO model of disilane (for Si_2H_6 orbital sketches see Figure 3).

ambiguous deconvolution of overlapping bands remains for the well-separated ones of trisilane and disilane (Figure 2). From their spectra two different interaction parameters $\beta^H{}_{SiSi/SiSi}$ would result within an LCBO MO model analogous to the one for methylsilanes (Figure 1), $IE_1(Si_3H_8) - IE_1(Si_2H_6) = 9.87 - 10.53 = -0.65$ eV and $IE_1(Si_2H_6) - IE_2(Si_3H_8) = 10.53 - 10.72 = -0.2$ eV, respectively. On the other hand, relative to the shifted trisilane center of gravity $IE_n(\sigma_{SiSi}) = 10.3$ eV an interaction parameter $(IE_1 - IE_2)/2 = -0.43$ eV $\equiv \beta^H{}_{SiSi/SiSi}$ is obtained, which corresponds reasonably to $\beta^{CH_3}{}_{SiSi/SiSi} = 0.5$ eV for the methylsilanes (Figure 1). Summarizing, the "σ_{SiSi} ionizations" of silanes are compressed with increasing energy, and therefore an LCBO MO model considering only σ_{SiSi} bond orbitals must fail in the interpretation. Obviously, any expansion of the model including unoccupied orbitals cannot explain the compression on the higher energy side of the "σ_{SiSi} ionization" region. On the contrary, the adjoining σ_{SiH} ionization humps in the PES (Figure 2) suggest—supported also by the results of the CNDO calculations (Figures 3-6)—that σ_{SiH} bond orbitals have to be included. A complete LCBO MO model for the simplest member of the series, disilane, and its parametrization using PE spectroscopic ionization energies justifies the above assumption.

PES Parametrization of LCBO MO Models for Disilane and Ethane. A complete LCBO MO model for disilane can be easily constructed from SiH_4 group orbitals and one SiSi bond orbital (Figure 9). The MO model construction and also its PE spectroscopic parametrization proceeds via joining of two SiH_3 units (Figure 9). Starting point is the σ_{SiH} bond orbital parameter $\sigma_{SiH} = -14.1$ eV, corresponding to the mean of the SiH_4 ionizations. For a SiH_3 fragment one deduces—assuming the same geminal interaction parameter $\beta^{gem}{}_{SiH/SiH} = -1.4$ eV—the group orbital energies $\alpha^e{}_{SiH_3} \approx -12.7$ eV and $\alpha^{a_1}{}_{SiH_3} \approx -16.8$ eV. Comparison with the disilane PE spectroscopic ionization energies (Table I) $1e_u$, $1e_g$, and $1a_{2u}$ leads to two internal parameters $\beta^e{}_{SiH_3/SiH_3} \sim -0.5$ eV and $\beta^{a_1}{}_{SiH_3/SiH_3} \sim -0.3$ eV. Using the latter, one obtains for the symmetric combination of six SiH bonds in $H_3Si\cdots SiH_3$ an internal coulomb parameter $\alpha^{a_{1g}}{}_{H_3Si\cdots SiH_3} \sim -17.1$ eV. Judging from the a_1 ionization of silane and assuming a symmetrical split $1a_{2u}/1a_{1g}$ for disilane, the $1a_{1g}$ ionization of Si_2H_6 might be found near 19.8 eV, corresponding to a stabilization of the $H_3Si\cdots SiH_3$ linear combination a_{1g} on SiSi bond admixture by about 2.7 eV. Subtracting this 2.7 eV difference from the first ionization energy of disilane $IE_1(2a_{1g}) = 10.53$ eV leads to the internal SiSi bond orbital parameter $\alpha_{SiSi} = -13.2$ eV. Finally, for the interaction between the only two disilane orbitals of a_{1g} symmetry, which represents within our model the admixture of SiH contributions to the

Table II. Comparison of LCBO MO Parameters for Disilane and Ethane

H_3XXH_3	α_{XX}	α_{XH}	$\beta^{gem}_{XH/XH}$	$\beta^{e}_{XH_3/XH_3}$	$\beta^{a_1}_{XH_3/XH_3}$	$\beta_{XX/XH}$
Si	−13.2	−14.1	−1.4	−0.5	−0.3	−1.7
C	−15.4	−16.4	−2.2	−1.2	−0.4	−2.4
C[11]	−15.6	−16.4	−2.2	−1.3[a]	−0.2[a]	−2.3

[a] Calculated from the parameters f and g given by Murrell and Schmidt[12] according to $\beta^{e}_{XH_3/XH_3} = f - g$ and $\beta^{a_1}_{XH_3/XH_3} = f + 2g$.

SiSi bond, the resonance integral $\beta_{SiSi/SiH}$ is calculated considering a normalization factor $1/\sqrt{6}$ as shown below (eq 2). Interesting results from the PE spectroscopic parametri-

$$\begin{vmatrix} \alpha_{SiSi} - \epsilon & \frac{6}{\sqrt{6}}\beta_{SiSi/SiH} \\ \frac{6}{\sqrt{6}}\beta_{SiSi/SiH} & \alpha^{a_1/g}_{H_3Si\cdots SiH_3} - \epsilon \end{vmatrix} = 0 \qquad (2)$$

$$\beta_{SiSi/SiH} = -\sqrt{\frac{(13.2 - 10.5)(17.1 - 10.5)}{6}} = -1.7 \text{ eV}$$

zation of the complete LCBO MO model for disilane are the estimated SiSi bond parameter $\alpha_{SiSi} = -13.2$ eV and the relatively strong SiH admixture as suggested by the interaction parameter $\beta_{SiSi/SiH} \sim -1.7$ eV. In this connection a comparison seems useful with the corresponding parameters of the iso(valence) electronic molecule ethane (Table II), determined analogously (Figure 9) from the PE ionization energies[9-12] of methane and ethane. Table II includes also the parameters evaluated independently by Murrell and Schmidt[12] from the PES of a larger number of alkanes based on ab initio calculations and on the LCBO MO model approach by Hall[13] and Brailford and Ford.[15] The agreement is almost perfect, and therefore lends some credit also to the disilane values. These reflect the smaller effective nuclear charge of silicon $|\alpha_{SiSi}| < |\alpha_{CC}|$ and the longer bond distances in disilane $|\beta_{X=Si}| < |\beta_{X=C}|$. In addition it should be mentioned that the missing silicon bond interaction parameter $\beta_{SiSi/SiSi} \sim -2$ eV[3] has been estimated in a way similar to Figure 9, but rather cumbersome from a trisilane LCBO MO model because the number of terms to be considered increases rapidly with molecular size. Anyhow, the $\beta_{SiSi/SiSi}$ is of no use in the discussion of n-tetrasilane and n-pentasilane because of their conformational ambiguity discussed above (Figure 5-7).

Some Remarks on Bond-Bond Interaction Models for Homologous Series of Compounds. To rationalize molecular properties of chemically related compounds MO models are often helpful: those which have been parametrized using PE ionization energies[31] and among others—especially for homologous series—those which incorporate chemical intuition by combining bond orbitals; see, for example, ref 5, 12-14, 25, 31-33. Therefore, the failure of a simple SiSi bond-bond interaction model for the silane series Si_nH_{2n+2} stimulates the question why for linear and cyclic methylsilanes $-[Si(CH_3)_2]_n-$ the first ionization energy of hexamethyldisilane can be used as an internal standard $\alpha^{CH_3}_{SiSi}$, around which the σ_{SiSi} ionization are split by $\beta^{CH_3}_{SiSi/SiSi} \sim -0.5$ eV according to the topology of the individual silicon skeleton (Figure 1). For n-$Si_4(CH_3)_{10}$, however, deconvolution of overlapping bands already reveals a deviation from the regression line (Figure 1) with differences in ionization energies $IE_2 - IE_1 = 0.7_8$ eV and $IE_3 - IE_2 = 0.5_4$ eV, respectively.[5] The PES of n-$Si_5(CH_3)_{12}$ (Figure 10), recorded in the meantime, further substantiates a "compression effect" also for the higher methylsilanes with $n \geq 4$. On the other hand, the first two separated PE bands of octamethyltrisilane show—within measurement accuracy—an equidistant split relative to the first one of hexamethyldisilane whereas for the corresponding silanes the center of gravity is shifted by −0.2 eV. Furthermore, the σ_{SiSi} ionization po-

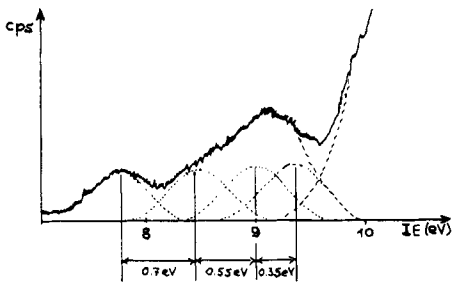

Figure 10. PES region 7-10 eV of n-$Si_5(CH_3)_{12}$ with band deconvolution.

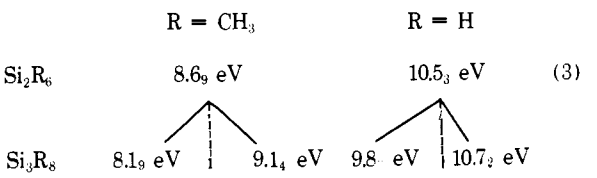

(3)

tentials of the cyclic methylsilanes $(Si(CH_3)_2)_n$ with $n = 5$, 6 fit in satisfactorily with the regression[5] in Figure 1.

The unsymmetrical σ_{SiSi} ionization patterns of $Si_4(CH_3)_{10}$ and especially of $Si_5(CH_3)_{12}$ can be explained to some extent assuming a conformer mixture as for the higher silanes Si_nH_{2n+2} with $n \geq 4$, although the larger interference radii of methyl groups probably counteract twisting around the SiSi axes. Nevertheless, additional effects must be considered to interpret the different splits (3) of individual conformers. An indication seems to be given by the different half-widths of the σ_{SiC} and σ_{SiH} ionization regions, $Si_3(CH_3)_8 \sim 1.4$ eV[5] and $Si_3H_8 \sim 2$ eV (Figure 2), respectively. This observation suggests for LCBO MO models different SiR-SiR interactions, i.e., $|\beta_{SiC/SiC}| < |\beta_{SiH/SiH}|$. An analogous assumption, that interactions SiSi-SiC are also smaller than those between SiSi and SiH bonds, and therefore can be neglected in a simplifying approximation, would help to explain, why the center of gravity of σ_{SiSi} ionizations is shifted differently (3) in the methylsilane and in the silane series.

Summarizing, simple bond-bond interaction models are a better approximation the more the molecules under consideration are structurally fixed, the higher their overall symmetry, and the better they can be subdivided into characteristic subunits—specifications, largely fulfilled for methylsilanes (Figure 1), but not for alkanes or silanes.

References and Notes

(1) Part L: H. Bock, K. Wittel, M. Veith, and N. Wiberg, *J. Am. Chem. Soc.*, **98**, 109 (1976). Also Part XXVII of "Contributions to the Chemistry of Silicon and of Germanium", for XXVI cf. F. Fehér and D. Skrodzki, *Inorg. Nucl. Chem. Lett.*, in press.
(2) Part of the thesis of W. Ensslin, University of Frankfurt, 1974.
(3) Part of the thesis of R. Freund, University of Cologne, 1973.
(4) Correspondence addresses (a) D-6 Frankfurt/M., Theodor-Stern-Kai 7; (b) Institute for Theoretical Chemistry, University, D-4 Düsseldorf, Ulenbergstr. 127; (c) D-5 Köln 1, Zülpicher Str. 47.

(5) H. Bock and W. Ensslin, *Angew. Chem.*, **83**, 435 (1971), *Angew. Chem., Int. Ed. Engl.*, **10**, 404 (1971).
(6) T. Koopmans, *Physica (Utrecht)*, **1**, 104 (1934). Cf. also E. Heilbronner in "The World of Quantum Chemistry", R. Daudel and B. Pullmann, Ed., D. Reidel Publishing Co, Dordrecht, Holland, 1974, pp 221-235.
(7) C. G. Pitt, M. M. Bursey, and P. F. Rogerson, *J. Am. Chem. Soc.*, **92**, 519 (1970), and literature quoted there.
(8) E. Carberry and R. J. West, *J. Organomet. Chem.*, **6**, 582 (1966).
(9) W. C. Price, *Mol. Spectrosc., Proc. Conf.*, 231 (1968); cf. also A. W. Potts and W. C. Price, *Proc. R. Soc. London, Ser. A*, **326**, 165 (1972).
(10) A. D. Baker, D. Betteridge, N. R. Kemp, and R. E. Körby, *J. Mol. Struct.*, **8**, 75 (1971).
(11) B. Narayan, *Mol. Phys.*, **23**, 281 (1972).
(12) J. N. Murrell and W. Schmidt, *J. Chem. Soc., Faraday Trans. 2*, 1709 (1972).
(13) G. G. Hall, *Proc. R. Soc. London, Ser. A*, **205**, 541 (1951).
(14) C. Sandorfy, *Can. J. Chem.*, **33**, 1337 (1955), or in O. Sinanoglu and K. B. Wiberg, "Sigma Molecular Orbital Theories", Yale University Press, New Haven, Conn., 1970.
(15) D. F. Brailford and B. Ford, *Mol. Phys.*, **18**, 621 (1970).
(16) W. W. Herndon, *Chem. Phys. Lett.*, **10**, 460 (1971).
(17) B. P. Pullen, T. A. Carlson, W. E. Moddeman, G. K. Schweitzer, W. E. Bull, and F. A. Grimm, *J. Chem. Phys.*, **53**, 768 (1970).
(18) S. Cradock, *J. Chem. Phys.*, **55**, 980 (1971).
(19) F. Feher, D. Schinkitz, V. Lwowski, and A. Oberthür, *Z. Anorg. Allg. Chem.*, **384**, 231 (1971).
(20) F. Feher, D. Schinkitz, and J. Schaaf, *Z. Anorg. Allg. Chem.*, **383**, 303 (1971).
(21) P. Hädicke, Thesis, University of Cologne, 1973.
(22) F. Fehér, G. Kuhlbörsch, and H. Luhleich, *Z. Anorg. Allg. Chem.*, **303**, 294 (1960); *Z. Naturforsch.*, **14b**, 466 (1959).
(23) F. Fehér, P. Hädicke, and H. Frings, *Inorg. Nucl. Chem. Lett.*, **9**, 931 (1973).
(24) J. Kroner, D. Proch, W. Fuss, and H. Bock, *Tetrahedron*, **28**, 1585 (1972).
(25) W. Ensslin, H. Bock, and G. Becker, *J. Am. Chem. Soc.*, **96**, 2757 (1974).
(26) The applicability of Lorentz and Gauss curves for ESCA spectra simulation has been tested; cf. K. Siegbahn, C. Nordling, G. Johansson, J. Hedman, P. F. Heden, K. Hamrin, U. Gelius, T. Bergmark, L. O. Werme, R. Manne, and Y. Baer "ESCA Applied to Free Molecules", North Holland Publishing Co, Amsterdam, 1970.
(27) M. S. Gordon and L. Neubauer, *J. Am. Chem. Soc.*, **96**, 5690 (1974), and literature quoted.
(28) B. Beagley, A. R. Conrad, J. M. Freemann, J. J. Monaghan, B. G. Norton, and G. C. Holywell, *J. Mol. Struct.*, **11**, 371 (1972).
(29) F. J. Wondarczyk and E. B. Wilson, *J. Chem. Phys.*, **56**, 166 (1972).
(30) W. England and M. S. Gordon, *J. Am. Chem. Soc.*, **93**, 4649 (1971), and literature quoted.
(31) Cf. the review by H. Bock and B. G. Ramsey, *Angew. Chem., Int. Ed. Engl.*, **12**, 734 (1973), containing numerous literature quotations.
(32) M. Beez, G. Bieri, H. Bock, and E. Heilbronner, *Helv. Chim. Acta*, **56**, 1028 (1973).
(33) Cf. the reveiw by H. Bock, *Int. J. Pure Appl. Chem.*, in press.

The Luminescence of Heterobischelated Complexes of Iridium(III). II. Analysis of the Thermally Nonequilibrated Levels in the Luminescence of *cis*-Dichloro(1,10-phenanthroline)(4,7-dimethyl-1,10-phenanthroline)iridium(III) Chloride

Richard J. Watts,* B. G. Griffith,[1] and J. S. Harrington

Contribution from the Department of Chemistry, University of California, Santa Barbara, Santa Barbara, California 93106. *Received May 9, 1975*

Abstract: The multiple emissions of *cis*-dichloro(1,10-phenanthroline)(4,7-dimethyl-1,10-phenanthroline)iridium(III) chloride, $[IrCl_2(phen)(4,7\text{-}Me(phen))]Cl$, have been resolved by analysis of luminescence decay curves as a function of emission wavelength. The data are best fit by a model which views the luminescence as the result of three sets of thermally nonequilibrated levels with lifetimes of 6.0, 8.7, and 22 μs. The levels all lie within a 400-cm^{-1} energy region. The 22-μs set of levels arises from a mixed $d\pi^*$-$\pi\pi^*$ orbital parentage localized around the 4,7-Me(phen) ligand. The 6.0 and 8.7 μs levels arise from $d\pi^*$ or d-d orbital parentage. The orbital parentage of the levels produced by excitation is retained to some degree during radiationless deactivation of the complex. The origin of this unique behavior in the heterobischelated complexes of Ir(III) is attributed to the combined effects of charge localization and vibrational deficiencies.

The nonexponential luminescence decay of *cis*-dichloro(1,10-phenanthroline)(5,6-dimethyl-1,10-phenanthroline)iridium(III) chloride, $[IrCl_2(phen)(5,6\text{-}Me(phen))]Cl$, at 77 K has been reported.[2] This molecule is the first example of an iridium(III) complex with this unusual property, which is indicative of emission of light from two or more sets of thermally nonequilibrated levels. The decay curves for this complex have been determined as a function of emission wavelength throughout the luminescence spectrum.[3] Analysis of these data on the basis of a model which presumes that two sets of thermally nonequilibrated levels are responsible for the emission indicates that the two sets of levels are split by 200-300 cm^{-1}. The lower set of levels decays with a lifetime of 65 μs and is thought to arise from $\pi\pi^*$ orbital parentage. The upper set decays with a lifetime of 9.5 μs and is thought to arise from $d\pi^*$ orbital parentage. The rate of interconversion of the two sets is thought to be negligible relative to their rates of decay to the ground state. From an analysis of the excitation wavelength dependence of the decay curves and time-resolved spectra of the complex we have formulated the following set of selection rules for radiationless transitions in the molecule: $d\pi^* \longleftrightarrow d\pi^*$; $\pi\pi^* \longleftrightarrow \pi\pi^*$; $d\pi^* \not\longleftrightarrow \pi\pi^*$. That is, there is a tendency toward retention of orbital parentage during radiationless deactivation of the complex.

The formulation of a set of symmetry-based selection rules for radiationless transitions in polyatomic molecules has been attempted by several authors.[4,5] Although these selection rules are of some utility, particularly in the case of small molecules with vibrational deficiencies,[5a] they are difficult to apply to large molecules. This difficulty arises from two major sources. First, the symmetry of the various excited states of large molecules is often not known with sufficient certainty to apply symmetry selection rules with confidence. Second, the abundance of vibrational modes of all possible symmetries in polyatomic molecules usually provides for a vibration of the right symmetry to make the radiationless transition between any two electronic levels al-